Random temporal connections promote network synchronization

Shijie Zhou,[1,2,3] Yao Guo,[1,4] Maoxing Liu,[5] Ying-Cheng Lai,[6] and Wei Lin[1,2,3,4,*]

[1]*Centre for Computational Systems Biology, Fudan University, Shanghai 200433, China*
[2]*School of Mathematical Science, Fudan University, Shanghai 200433, China*
[3]*Shanghai Center of Mathematical Sciences, Shanghai 200433, China*
[4]*Institute of Science and Technology for Brain-Inspired Intelligence, Fudan University, Shanghai 200433, China*
[5]*Department of Mathematics, North University of China, Taiyuan 030051, China*
[6]*School of Electrical, Computer, and Energy Engineering, Arizona State University, Tempe, Arizona 85287-5706, USA*

(Received 25 November 2018; revised manuscript received 20 August 2019; published 4 September 2019)

We report a phenomenon of collective dynamics on discrete-time complex networks: a random temporal interaction matrix even of zero or/and small average is able to significantly enhance synchronization with probability one. According to current knowledge, there is no verifiably sufficient criterion for the phenomenon. We use the standard method of synchronization analytics and the theory of stochastic processes to establish a criterion, by which we rigorously and accurately depict how synchronization occurring with probability one is affected by the statistical characteristics of the random temporal connections such as the strength and topology of the connections as well as their probability distributions. We also illustrate the enhancement phenomenon using physical and biological complex dynamical networks.

DOI: 10.1103/PhysRevE.100.032302

I. INTRODUCTION

Collective dynamics on complex networks such as synchronization and stability [1–24] are a central theme in network science and engineering. Most previous studies concerned mainly static networks, i.e., networks whose structures are fixed in time. Static networks, however, represent only an approximate description of the real world—networks arising in biological, physical, and social systems are often time varying or temporal [25–35]. Collective dynamics on temporal networks, in spite of their importance, were far less studied. In this regard, there was a line of work on synchronization and stability in temporal networks [10,32,36–51]. For example, moving agent networks were studied [36,37,41,45], where interactions among the agents are switched on when they are sufficiently close in the physical space. A result was that, if all agents are moving randomly, there exists an interval in the agent density in which synchronization can be achieved and this interval does not depend on the network size [36,37]. An alternative setting is a fixed set of zones: only when agents enter into one of these zones will interactions be activated [45]. In this case, the network synchronizability depends on the system size in that synchronization is more difficult for larger systems, which can be quantified by an algebraic scaling law [45]. The problem of synchronization and stability in temporal networks has potential applications in applied fields such as wireless communication and intelligent robotics.

A key previous result on synchronization in temporal networks is that the expectation value of nodal interaction or coupling strength in the network must be nonzero and even sufficiently large to achieve global synchrony [10,39,45,46,49]. This result agrees with intuition because, when the nodal interactions are randomly varying with time, a certain amount of average coupling is required for any coherent behavior to emerge in the network. In this article, we address the following questions: "Is there any phenomenon that is different from the previous result?" and "Can synchronization be achieved on temporal networks with probability one, or equivalently, in a physical sense even when the expectation value of the coupling in the network is fairly small or even zero?" Affirmative answers to these questions will indicate that, comparing with the case of a static network, interaction matrices that are switched in a completely random manner, even with zero or/and small average, are sufficient to enhance network synchronization with probability one.

Although there have been numerous results on the positive role of additive or multiplicative noise with zero mean to induce the emergence of a variety of physical phenomena, including stochastic resonances [52], state transitions [53], and stochastic synchronization [54], the underlying systems are described by continuous-time dynamical systems. Comparing with the infinitesimal step size or fast switching in the continuous-time systems, the constant step size or the slow iteration character hampers the positive role of randomness in discrete-time systems that are broadly adopted in modeling and in computations. Thus analytical and numerical advances on the enhancement of collective dynamics of random temporal networks in a discrete-time mode are rare, only including the recent result [55] which presents necessary conditions for the enhancement phenomena in a probability moment sense, requiring further improvement. According to the theory of probability and stochastic processes, results in the moment sense do not imply results emergent with probability one. In this article, we establish the necessary and sufficient conditions for the emergence of synchronization with probability

*wlin@fudan.edu.cn

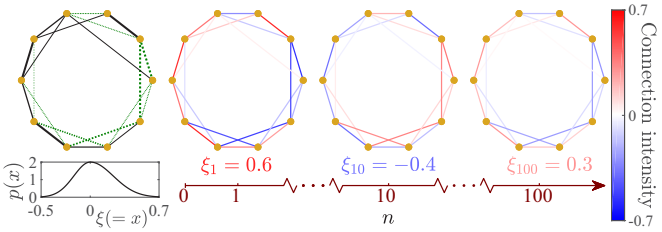

FIG. 1. Snapshots of a random temporal network. The solid and dashed lines indicate connections of positive and negative strength, respectively. A unimodal probability distribution $p(x)$ for the random variable ξ is also shown.

one through rigorous mathematical analyses and test it by using realistic biological and physical networks. An implication is that, in dynamical networks from the real world even with discrete-time modes, randomness not in the traditional sense of additive noises on the dynamical variables but in the temporal and multiplicative variations of the network interactions can be beneficial to the emergence and enhancement of desired collective dynamics.

II. NETWORK MODELS AND SYNCHRONIZATION STABILITY CONDITION

We begin by considering a discrete-time dynamical network of N nodes, each represented by the dynamical variable θ^i $(i = 1, 2, \ldots, N)$:

$$\theta^i(n+1) = f(\theta^i(n)) + \sum_{j\neq i}^{N} \alpha_{ij}[f(\theta^j(n)) - f(\theta^i(n))] + \sum_{j\neq i}^{N} g_{ij}\xi_n[f(\theta^j(n)) - f(\theta^i(n))], \quad (1)$$

where the nonlinear map $f(\cdot)$ describes the individual nodal dynamics, and α_{ij} and g_{ij} characterize the deterministic (fixed) and randomly time-varying connections in the network, respectively, with ξ_n being the temporal realizations of a random variable ξ following a given probability distribution. We assume that ξ can take zero mean: $\mathbb{E}(\xi) = 0$. A number of examples of temporal realizations (snapshots) of the network are illustrated in Fig. 1. The temporal structure described by the third term in Eq. (1) can be regarded as due to the random environmental fluctuations in biological or physical systems.

We first examine the case where the deterministic connections are absent: $\alpha_{ij} = 0$. For concreteness, we assume that the individual nodal dynamical system is described by a one-dimensional map having a global stable or chaotic attractor and the network matrix $\boldsymbol{G} = \{g_{ij}\}$ with $g_{ii} = -\sum_{j\neq i}^{N} g_{ij}$ is diagonalizable:

$$\boldsymbol{G} = \boldsymbol{P}^{-1}\mathrm{diag}\{\lambda_1, \ldots, \lambda_N\}\boldsymbol{P},$$

where $\boldsymbol{P} = \{p_{ij}\}$ is a row-normalized transformation matrix and λ_i $(i < N)$ are the complex eigenvalues that are distinct from the trivial eigenvalue $\lambda_N = 0$. In this setting, the state of system (1) in the synchronization manifold is

$$\overline{\theta}(n) = \sum_{j=1}^{N} p_{Nj}\theta^j(n), \quad \overline{\theta}(n+1) = \sum_{j=1}^{N} p_{Nj}f(\theta^j(n)),$$

where $p_{Nj} = 1/N$ for all j if $\boldsymbol{G}$ is symmetric. The synchronization error $e(n) = \theta^i(n) - \overline{\theta}(n)$ is governed by the linearized dynamical evolution:

$$e^i(n+1) = f'(\overline{\theta}(n))\left[e^i(n) + \sum_{j=1}^{N} g_{ij}\xi_n e^i(n)\right].$$

Letting $[q^1(n), \ldots, q^N(n)]^\top = \boldsymbol{P}[e^1(n), \ldots, e^N(n)]^\top$, we obtain a set of variational equations:

$$q^i(n+1) = f'(\overline{\theta}(n))[q^i(n) + \lambda_i\xi_n q^i(n)]$$

for $i = 1, \ldots, N$. The theory of master stability function [56–59] stipulates that the asymptotical stability of the variational equations associated with the nontrivial eigenvalues $\lim_{n\to\infty} q^i(n) = 0$ for all $i < N$ guarantees the emergence of local synchronization. We thus seek to establish a condition for asymptotical stability of the generic variational equation:

$$q(n+1) = f'(\overline{\theta}(n))[q(n) + \lambda\xi_n q(n)],$$

which governs the evolution of an infinitesimal perturbation q transverse to the synchronization manifold. Taking logarithm and using inductive calculations, we get

$$\ln|q(n+1)| = \ln|f'(\overline{\theta}(n))| + \ln|1 + \lambda\xi_n| + \ln|q(n)| = \ln|q(1)| + \sum_{k=1}^{n}\ln|1+\lambda\xi_k| + \sum_{k=1}^{n}\ln|f'(\overline{\theta}(k))|.$$

Thus the exponential growth rate of $q(n)$, defined as $S(q(n)) = (1/n)\ln|q(n)|$, is given by

$$S(q(n)) = \frac{S(q(1))}{n+1} + \sum_{k=1}^{n}\frac{\ln|1+\lambda\xi_k|}{n+1} + \sum_{k=1}^{n}\frac{\ln|f'(\overline{\theta}(k))|}{n+1}.$$

The strong law of large numbers [60] and the ergodic theory of chaotic dynamical systems [61] give

$$\lim_{n\to\infty} S(q(n)) = \mathbb{E}(\ln|1+\lambda\xi|) + \lambda^L$$

almost surely, where "almost surely" refers to "with probability one" or "in a physical sense," $\mathbb{E}(\cdot)$ is the expectation, and λ^L is the Lyapunov exponent of f in the synchronization manifold. The necessary and sufficient condition for the asymptotical stability with probability one is thus given by [ASC],

$$\mathbb{E}(\ln|1+\lambda\xi|) < -\lambda^L,$$

which further leads to a condition for local asymptotical synchronization to emerge with probability one in the networked system (1): $\mathbb{E}(\ln|1+\lambda_i\xi|) < -\lambda^L$ for all $i < N$ [SEC]. In the special case where ξ is deterministically set as unity and the Lyapunov exponent λ^L is positive, the condition [SEC] can be violated if the transverse spectrum λ_i has both positive and negative eigenvalues. However, if ξ is random, some appropriate choice of its distribution is able to induce synchronization. More importantly, the above arguments indicate that, in discrete-time systems, the real strength of the random

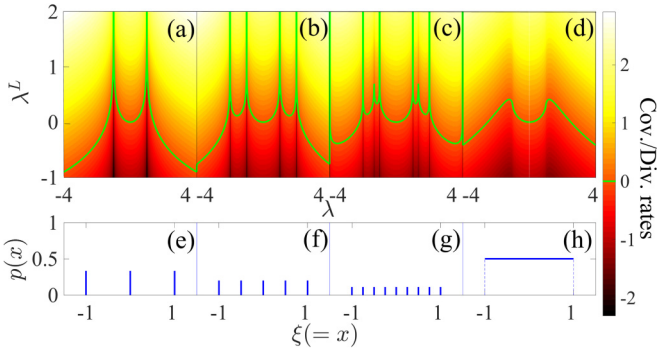

FIG. 2. Emergence of synchronization in temporal networks with randomly varying connections governed by discrete or uniform probability distributions. Shown are the stability regions fulfilling the condition [ASC] in the λ-λ^L plane for different probability distributions. In (a)–(d), the regions are below the highlighted boundaries [solid (green) curves], and the colors represent the values of the exponentially convergent or divergent rates. The distributions in (e)–(g) are with discrete values with identical probability, while the distribution in (h) takes on an infinite number of continuous values with a uniform probability.

interactions cannot be counted directly as the expectation of the interaction matrix *per se*, while it should be interpreted as the expectation of its logarithm forms in the conditions [ASC] and [SEC]. Observing the influence of the logarithm terms is also consistent with the conventional requirement of the classical results on the convergence in discrete-time systems.

III. SYNCHRONIZATION STABILITY CONDITION ANALYTICS: FROM DISCRETE-VALUED DISTRIBUTION TO CONTINUOUS-VALUED DISTRIBUTION

We derive the criteria for selecting synchronization-enabling probability distribution. For simplicity, we drop the superscript i and focus on the condition [ASC]. Consider the case where the zero-mean random variable ξ takes on discrete values x_j with the corresponding probabilities p_j $(j = 1, \ldots, v)$. The condition [ASC] becomes

$$\sum_{j=1}^{v} p_j \ln|1+\lambda x_j| < -\lambda^L.$$

To be concrete, we let x_j take on values from the set of finite elements: $\{-1, \ldots, -1+2^{-k}, -1+2^{1-k}, \ldots, 1\}$ with identical probability $p_j \equiv p = (2^{k+1}+1)^{-1}$ and real-valued transversal eigenvalue λ. As shown in Fig. 2(a), a region of twin towers of an infinite height, which fulfills [ASC], appears in the λ-λ^L plane for the distribution of $k = 0$ [Fig. 2(e)]. The region is above the line $\lambda^L = 0$, manifesting that just random temporal connections are sufficient for achieving synchronization. Figures 2(b) and 2(c) show a rapid growth in the number of towers as k increases to larger values [e.g., $k = 2, 3$ in Figs. 2(f) and 2(g)]. When $p(x)$ becomes a continuous-valued distribution, the towers disappear abruptly and small twin towers appear, as shown in Figs. 2(d) and 2(h), where ξ follows a uniform distribution. We thus see that continuous-valued random variables lead to bounded and smaller stability regions in the λ-λ^L plane, while discrete random variables yield unbounded stability regions.

Consider the case where ξ follows the Cauchy-Lorentz distribution [62,63]:

$$p(x) = c\frac{1}{\pi}\frac{1}{c^2+(x-d)^2}$$

with $c > 0$. For this unimodal and continuous-valued distribution, using the theorem of residues [64] and the calculations presented in the Appendix makes the condition [ASC] become

$$\mathbb{E}(\ln|1+\lambda\xi|) = \int_{-\infty}^{+\infty} \ln|1+\lambda x| p(x)dx = \mathrm{Re}\{\ln[1+\lambda(d \pm ic)]\} < -\lambda^L, \quad (2)$$

where $\mathrm{Re}\{\cdot\}$ is an operator taking the real part of a given number. For a real-valued transverse eigenvalue λ, the condition in (2) becomes

$$\ln\sqrt{(1+\lambda d)^2+\lambda^2 c^2} < -\lambda^L.$$

Specifically, for $d = 0$, which corresponds to a distribution centered at the origin with zero expectation, we get $\ln\sqrt{1+\lambda^2 c^2} < -\lambda^L$. However, this condition fails, regardless of the network topology, when the dynamics in the synchronization manifold are chaotic (i.e., $\lambda^L > 0$). The tenability of the condition is guaranteed only for nonzero values of d (nonzero expectation). For example, if $d > 0$, [ASC] holds for some appropriately selected negative λ and sufficiently small c satisfying the relation $(1+\lambda d)^2+\lambda^2 c^2 \ll 1$. For a symmetric network $\boldsymbol{G}$ with positive elements g_{ij} $(i \neq j)$, all transverse eigenvalues λ_i are negative, giving rise to the remarkable phenomenon that random temporal connections lead to the emergence of local synchronization.

Now consider the case where ξ obeys a bimodal probability distribution:

$$h(x) = \frac{1}{2\pi}\left[\frac{c_1}{c_1^2+(x-d)^2} + \frac{c_2}{c_2^2+(x+d)^2}\right],$$

where $c_{1,2}$ with $c_1 + c_2 = 2$ are the widths of the two peaks in h and $2d > 0$ is the distance between the two peaks. This distribution is symmetric with zero mean [65] for $c_{1,2} = 1$. Following the analysis with the unimodal distribution, we obtain [ASC] as

$$\mathbb{E}(\ln|1+\lambda\xi|) = \int_{-\infty}^{+\infty} \ln|1+\lambda x| h(x)dx = \frac{1}{2}\mathrm{Re}\{\ln\{[1+\lambda(d \pm ic_1)][1+\lambda(-d \pm ic_2)]\}\} < -\lambda^L. \quad (3)$$

For real-valued λ, condition (3) becomes

$$\ln\left[\sqrt{(1+\lambda d)^2+c_1^2\lambda^2}\sqrt{(1-\lambda d)^2+c_2^2\lambda^2}\right] < -\lambda^L,$$

which generates a stability region in the λ-λ^L plane. As the peak-to-peak distance $2d$ is increased, the region contracts horizontally and stretches vertically, as shown in Figs. 3(a), 3(b), 3(e), and 3(f). We also find that, if the distribution h is asymmetric, the stability region becomes asymmetric as well but in the opposite order. Compared with the symmetric case, we have that the inequality $c_1 < c_2$ $(c_1 > c_2)$ allows λ^L to have

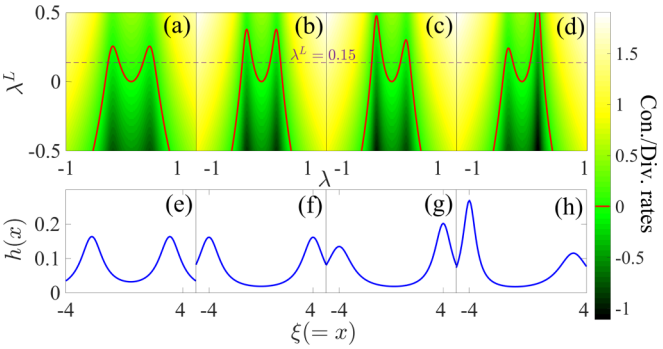

FIG. 3. Emergence of synchronization in temporal networks with randomly varying connections governed by continuous probability distributions. Shown are the stability regions in which the condition [ASC] holds in the λ-λ^L plane for different bimodal distributions of the random connection variable ξ. The solid (red) curves in (a)–(d) and the color bar have the same meanings as in Fig. 2. The distributions in (e) and (f) are symmetric but with different peak distances, and the distributions with $c_1 < c_2$ (g) and $c_1 > c_2$ (h) are asymmetric with their higher peaks at different loci.

a larger selection range for networks whose matrix $\boldsymbol{G}$ has real $\lambda < 0$ ($\lambda > 0$), as shown in Figs. 3(c), 3(d), 3(g), and 3(h).

To gain further insights, we investigate the condition [ASC] for complex-valued λ. As shown in Fig. 4, for $\lambda^L = 0.15$, two leaflike stability regions in λ arise separately in the complex plane. The two regions are symmetric only for $c_{1,2} = 1$, for which a larger value of d results in larger areas of the regions with a shorter distance between them, as shown in Fig. 4(a). Making the distribution h asymmetric will expand one region but shrink the other, as shown in Fig. 4(b), implying that a smaller value of c_1 with $c_1 < c_2$ enables a diagonalizable network matrix $\boldsymbol{G}$ with positive elements g_{ij} ($i \neq j$) to have a larger spectrum gap, i.e., a longer distance between the largest and the smallest norms of the transverse eigenvalues.

IV. PHYSICAL AND BIOLOGICAL EXAMPLES

We can now address the key question of whether and how randomly varying connections can induce global synchronization in physical or biological networks whose deterministic version does not permit synchronization.

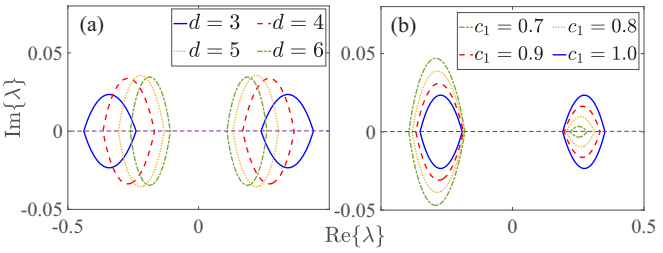

FIG. 4. Stability condition for complex eigenvalues. Shown are the stability regions satisfying the condition (3) in the complex plane of λ for $\lambda^L = 0.15$: (a) $c_{1,2} = 1$ and (b) $d = 3$. The horizontal dashed line coinciding with the real axis corresponds to the dashed line $\lambda^L = 0.15$ in Figs. 3(a)–3(d).

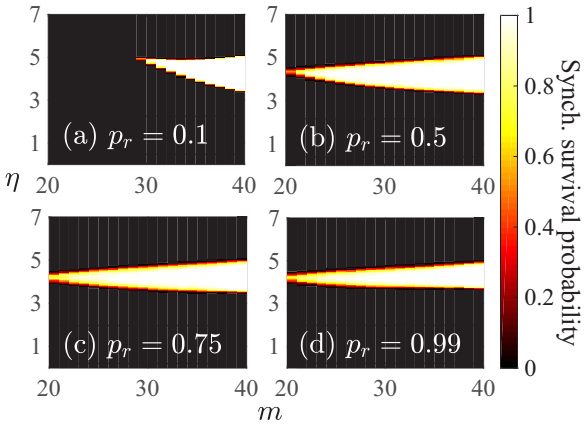

FIG. 5. Random connection induced synchronization in a small-world network of liquid-crystal spatial light modulators. Shown are the synchronization probability versus the strength η of randomly varying connections and m for different values of the reconnection probability p_r. The system parameters are $a = 4.7$ and $K = 0.1$, and the Lyapunov exponent of the individual nodal dynamics is $\lambda^L \approx 0.25$. The probability is calculated using 100 realizations of the small-world network, each of size $N = 100$.

The first example is an experimental liquid-crystal spatial light modulator with a spatially dependent phase shift [66]. A possible relation between the phase shift and the captured light, as generated by optical polarization, is a nonlinear map given, e.g., by

$$f(\theta) = \frac{a}{2}(1 - \cos\theta).$$

Assuming that the deterministic network has a small-world structure of one-dimensional lattice, we have in system (1) $\alpha_{ij} = [(1/(2m)]Ks_{ij}$, $g_{ij} = [1/(2m)]s_{ij}$, where K is the deterministic coupling strength, $s_{ij} \in \{0, 1\}$, and the connection matrix $\boldsymbol{S} = \{s_{ij}\}$ is symmetric with p_r being the reconnecting probability and $2m$ the number of nearest neighboring nodes before reconnection [67]. Random fluctuations are described by $\xi_n = \eta\zeta_n$, where η is the fluctuation intensity and all ζ_n independently obey a distribution that takes on the values ± 0.2 with equal probability. For $\eta \sim 0$, there is no synchronization, as shown in Fig. 5. Interestingly, when we turn on the value of η from zero, synchronization emerges. In particular, for the values of η and m in an ivorylike region, the synchronization probability is greater than 50% and can even reach unity, as shown in Fig. 5. We have verified the phenomenon directly and analytically through the condition [ASC] by exploiting the matrix spectrum $\boldsymbol{S}$ of small-world networks [68]. As shown in Fig. 5, the synchronization region is also dependent on the reconstructing probability p_r. We find that an optimal value of p_r in (0, 1) can maximize the area of the ivorylike stability region.

Our second example is a neuronal network for which the nodal dynamical system is two dimensional:

$$\boldsymbol{x}^i(n+1) = \boldsymbol{f}(\boldsymbol{x}^i(n)) + \sum_{j \neq i}^{N} a_n^{ij}[\boldsymbol{f}(\boldsymbol{x}^j(n)) - \boldsymbol{f}(\boldsymbol{x}^i(n))],$$

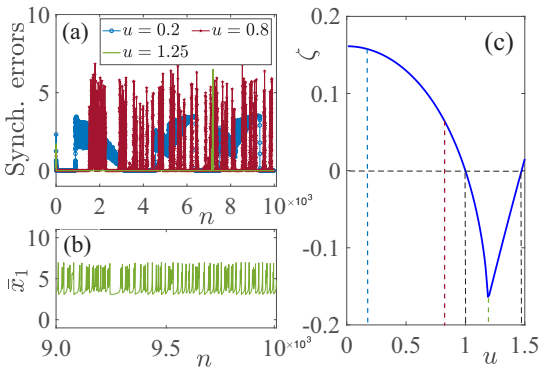

FIG. 6. Random connection induced emergence of synchronization in a neuronal network. (a) Synchronization error $[1/(N-1)]\sum_{i\neq 1}\|\boldsymbol{x}^1(n)-\boldsymbol{x}^i(n)\|$ in time for different values of the half fluctuation band u. (b) Synchronized spiking dynamics of the membrane potential variable of the mean field. (c) Minimization of the quantity ζ corresponding to the value of u in (a).

where $\boldsymbol{f}(\boldsymbol{x})=[4.9(1+x_1^2)^{-1}+x_2, x_2-0.001(x_1+1)]^\top$ describes the dynamics of an individual neuron [69]. The network has size $N=100$ with connection matrix elements given by $a_n^{ij}=[1/(2m)](K+\xi_n)s_{ij}$, where the matrix $\boldsymbol{S}=\{s_{ij}\}$ defines a small-world network and ξ_n is uniformly distributed in $[-u,u]$. Figure 6(a) shows that the synchronization error diminishes as the value of u is increased from zero to about 1.25. The synchronized spiking dynamics of $\bar{x}_1(n)$ are shown in Fig. 6(b), where $\bar{\boldsymbol{x}}(n)=(1/N)\sum_{i=1}^N \boldsymbol{x}^i(n)$ is the membrane potential of the mean field. The variational equations with respect to the synchronization manifold are

$$\boldsymbol{q}(n+1)=\nabla\boldsymbol{f}(\bar{\boldsymbol{x}}(n))[1+(K+\xi_n)\lambda_j]\boldsymbol{q}(n),$$

where $\nabla\boldsymbol{f}$ is the Jacobian matrix of $\boldsymbol{f}$ and λ_j is the transverse eigenvalue of the matrix $\boldsymbol{S}/(2m)$. The quantity

$$\zeta=\max_j\left\{\mathbb{E}[\ln|1+\lambda_j(K+\xi)|]+\lambda_{\max}^L\right\}<0$$

can be used to characterize the synchronization stability, where $\lambda_{\max}^L$ is the largest Lyapunov exponent of f in the synchronization manifold $\mathcal{M}$. As shown in Fig. 6(c), we have $\zeta<0$ for $u\in(1.00,1.47)$ and it approaches a minimum for $u\approx 1.25$. That is, as the random variations in the network connections (even of zero expectation) are tuned up, synchronization emerges.

V. CONCLUDING REMARKS

To summarize, we find that making the interaction matrix within a network randomly varying with discrete-time iterations, even when the expectation value of its random variations is fairly small or/and zero, can enhance or induce synchronization with probability one which otherwise would not possible either in a static setting or in a deterministic temporal setting. Our mathematical analysis and demonstration using physical and biological networks suggest that the finding holds generally true for different types of network topologies and distributions of the interactions. A combination of randomness and temporal variations in the structure of a network, not in the traditional sense of additive random noises, thus has the benefit of promoting synchronization, a type of collective dynamics that are relevant to networks in a variety of natural and engineering systems.

Moreover, since finding optimal parameters in machine learning and solving continuous-time systems or complex networks usually require discrete-time iteration algorithms, our findings can be beneficial to promoting the computational performance of these algorithms when particular forms of randomness are taken into account. Also, as the iteration step size becomes infinitesimal, the stability condition derived from the discrete-time algorithm could become the stability condition for the continuous-time systems, which provides an alternative way to depict how particular forms of randomness promote synchronization emergent in continuous-time complex networks. Additionally, the uncoupled nodal dynamics are supposed to be all identical in the above discussions; however, the method developed in the current article, with standard continuum techniques for investigating synchronization of Kuramoto's oscillators [63], can be further generalized to find synchronization-enabling randomness for networks with nodal dynamics of a heterogeneous nature. All these become our present or/and future research topics.

ACKNOWLEDGMENTS

W.L. is supported by LMNS, LCNBI, the National Science Foundation of China (NSFC) Grants No. 11322111 and No. 61773125, and the National Key R&D Program of China Grant No. 2018YFC0116600. Y.-C.L. is supported by the Office of Naval Research through Grant No. N00014-16-1-2828. M.L. is supported by the NSFC Grants No. 11571324 and No. 11331009.

S.Z., Y.G., and M.L. contributed equally to this work.

APPENDIX: EVALUATION OF AN INTEGRAL ARISING FROM SYNCHRONIZATION STABILITY ANALYSIS

In our mathematical analysis of synchronization stability of randomly time-varying networks, the following integral arises:

$$\mathbb{E}(\ln|1+\lambda\xi|)=\int_{-\infty}^{+\infty}\ln|1+\lambda x|p(x)dx,$$

where the singularity of the function $\ln(1+\lambda z)$ of complex variable z is located either on the upper (lower) half of the complex plane (case A) or on the real axis (case B).

For case A, we calculate the integral inside a semicircle, denoted by $\Gamma_R=[-R,R]\cup C_R$, on the complex plane:

$$\oint_{\Gamma_R}\ln(1+\lambda z)p(z)dz=\left\{\int_{-R}^{R}+\int_{C_R}\right\}\ln(1+\lambda z)p(z)dz,$$

where the curve C_R is set on the lower (upper) half of the complex plane if the singularity of $\ln(1+\lambda z)$ is on the upper (lower) half of the plane. According to the theorem of residues, we obtain that the value of the integral is $\ln[1+\lambda(d\pm ic)]$ for sufficiently large R. The second integral goes to zero in the limit of large R. Letting $R\to+\infty$, we have

$$\int_{-\infty}^{+\infty}\ln|1+\lambda x|p(x)dx=\mathrm{Re}\{\ln[1+\lambda(d\pm ic)]\},$$

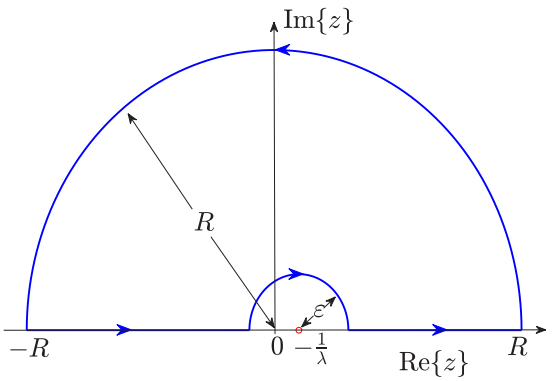

FIG. 7. Integral region circumscribed by the directional and closed curve $\Gamma_{R,\varepsilon} = [-\frac{1}{\lambda} + \varepsilon, R] \cup C_R \cup [-R, -\frac{1}{\lambda} - \varepsilon] \cup \gamma_\varepsilon$.

where Re{·} is an operator taking the real part of a given number.

For case B, assuming that the singularity $z = -1/\lambda$ ($\lambda \neq 0$) is on the real axis, we analyze the function $\ln(1 + \lambda z)$ of z inside the region

$$\mathcal{G} = \left\{ z \in \mathbb{C} : z \neq -\frac{1}{\lambda}, \quad -\frac{\pi}{2} < \arg\left(z + \frac{1}{\lambda}\right) < \frac{3\pi}{2} \right\},$$

where arg(·) is an operator taking the argument of a given complex number. Since $z = -1/\lambda$ is on the real axis, λ is a real number. Suppose we have

$$z + \frac{1}{\lambda} = \left| z + \frac{1}{\lambda} \right| e^{i\theta},$$

with $-\frac{\pi}{2} < \theta < \frac{3\pi}{2}$. We let

$$\ln(1 + \lambda z) = \ln(\lambda) + \ln\left| z + \frac{1}{\lambda} \right| + i\theta,$$

where we define $\ln(\lambda) = \ln|\lambda| + i\pi$ for $\lambda < 0$ and $\ln(\lambda)$ uses its regular definition for $\lambda > 0$.

Denote by $\Gamma_{R,\varepsilon}$ a closed curve in the complex plane, as shown in Fig. 7. Integration of the function $\ln(1 + \lambda z)p(z)$ along this closed curve can be separated into four parts:

$$\oint_{\Gamma_{R,\varepsilon}} \ln(1 + \lambda z)p(z)dz = \left\{ \int_{-\frac{1}{\lambda}+\varepsilon}^{R} + \int_{C_R} + \int_{-R}^{-\frac{1}{\lambda}-\varepsilon} + \int_{\gamma_\varepsilon} \right\} \ln(1 + \lambda z)p(z)dz, \quad \text{(A1)}$$

where C_R is a counterclockwise semicircle from R to $-R$ and γ_ε is a clockwise semicircle centered at $-1/\lambda$ from $-1/\lambda - \varepsilon$ to $-1/\lambda + \varepsilon$.

To evaluate the integrals in Eq. (A1), we first have

$$\int_{C_R} \ln(1 + \lambda z) \frac{c}{\pi[c^2 + (z - d)^2]} dz = \int_0^\pi \ln(1 + \lambda R e^{i\theta}) \frac{ci\theta}{\pi[c^2 + (R e^{i\theta} - d)^2]} R e^{i\theta} d\theta,$$

where

$$\left| \ln(1 + \lambda R e^{i\theta}) \frac{ci\theta}{\pi[c^2 + (R e^{i\theta} - d)^2]} R e^{i\theta} \right| \leqslant \frac{cR[\ln(1 + R|\lambda|) + 2\pi]}{(R - |d|)^2 - c^2}.$$

In the limit $R \to +\infty$, the estimate tends to zero, yielding

$$\int_{C_R} \log(1 + \lambda z) \frac{c}{\pi[c^2 + (z - d)^2]} dz \to 0$$

for $R \to +\infty$.

Secondly, we evaluate the integral

$$\int_{\gamma_\varepsilon} \ln(a + \lambda z)p(z)dz = \int_\pi^0 \varepsilon \ln(\lambda\varepsilon e^{i\theta}) p\left(-\frac{1}{\lambda} + \varepsilon e^{i\theta}\right) i e^{i\theta} d\theta.$$

Using the boundedness of the probability distribution $p(z)$ in the neighborhood of $z = -1/\lambda$ and the property of $\varepsilon \ln(\lambda\varepsilon e^{i\theta}) \to 0$ for $\varepsilon \to 0+$, we have

$$\int_{\gamma_\varepsilon} \ln(1 + \lambda z)p(z)dz \to 0$$

for $\varepsilon \to 0+$.

In the upper half of the complex plane, the function $\ln(1 + \lambda z)p(z)$ has a unique pole: $z = d + ic$. The theorem of residues gives

$$\int_{\Gamma_{R,\varepsilon}} \ln(1 + \lambda z)p(z)dz = \ln[1 + \lambda(d + ic)]$$

for sufficiently large R and sufficiently small ε. Consequently, letting $R \to +\infty$ and $\varepsilon \to 0+$ in Eq. (A1), we get

$$\int_{-\infty}^{+\infty} \ln(1 + \lambda z)p(z)dz = \ln[1 + \lambda(d + ic)]. \quad \text{(A2)}$$

Finally, taking the real parts of both sides of Eq. (A2), we obtain

$$\mathbb{E}(\ln|1 + \lambda\xi|) = \int_{-\infty}^{+\infty} \ln|1 + \lambda x|p(x)dx = \ln\sqrt{(1 + \lambda d)^2 + \lambda^2 c^2}.$$

This result agrees with that obtained above for case A where the singularity of $\ln(1 + \lambda z)$ is not located on the real axis.

[1] B. Blasius, A. Huppert, and L. Stone, Nature (London) **399**, 354 (1999).

[2] L. F. Lago-Fernandez, R. Huerta, F. Corbacho, and J. A. Siguenza, Phys. Rev. Lett. **84**, 2758 (2000).

[3] P. M. Gade and C.-K. Hu, Phys. Rev. E **62**, 6409 (2000).

[4] J. Jost and M. P. Joy, Phys. Rev. E **65**, 016201 (2001).

[5] M. Barahona and L. M. Pecora, Phys. Rev. Lett. **89**, 054101 (2002).

[6] X. F. Wang and G. Chen, Int. J. Bifurcat. Chaos Appl. Sci. **12**, 187 (2002).

[7] X. F. Wang and G. Chen, IEEE Trans. Circuits Syst. I **48**, 641 (2001).

[8] H. Hong, M. Y. Choi, and B. J. Kim, Phys. Rev. E **65**, 026139 (2002).
[9] T. Nishikawa, A. E. Motter, Y.-C. Lai, and F. C. Hoppensteadt, Phys. Rev. Lett. **91**, 014101 (2003).
[10] V. Belykh, I. Belykh, and M. Hasler, Physica D **195**, 159 (2004).
[11] I. Belykh, M. Hasler, M. Lauret, and H. Nijmeijer, Int. J. Bifurcat. Chaos **15**, 3423 (2005).
[12] L. Donetti, P. I. Hurtado, and M. A. Muñoz, Phys. Rev. Lett. **95**, 188701 (2005).
[13] C. Zhou and J. Kurths, Phys. Rev. Lett. **96**, 164102 (2006).
[14] C. Zhou and J. Kurths, Chaos **16**, 015104 (2006).
[15] K. Park, Y.-C. Lai, S. Gupte, and J.-W. Kim, Chaos **16**, 015105 (2006).
[16] L. Huang, K. Park, Y.-C. Lai, L. Yang, and K. Yang, Phys. Rev. Lett. **97**, 164101 (2006).
[17] X. G. Wang, L. Huang, Y.-C. Lai, and C.-H. Lai, Phys. Rev. E **76**, 056113 (2007).
[18] S.-G. Guan, X.-G. Wang, Y.-C. Lai, and C. H. Lai, Phys. Rev. E **77**, 046211 (2008).
[19] M. D. Holland and A. Hastings, Nature (London) **456**, 792 (2008).
[20] E. E. Goldwyn and A. Hastings, Theor. Popul. Biol. **73**, 395 (2008).
[21] E. E. Goldwyn and A. Hastings, Bull. Math. Biol. **71**, 130 (2009).
[22] Y.-Y. Liu, J.-J. Slotine, and A.-L. Barabási, Nature (London) **473**, 167 (2011).
[23] Y.-Y. Liu and A.-L. Barabási, Rev. Mod. Phys. **88**, 035006 (2016).
[24] Y.-Z. Sun, S.-Y. Leng, Y.-C. Lai, C. Grebogi, and W. Lin, Phys. Rev. Lett. **119**, 198301 (2017).
[25] S. A. Navarrete and E. L. Berlow, Ecol. Lett. **9**, 526 (2006).
[26] P. Holme and J. Saramäki, Phys. Rep. **519**, 97 (2012).
[27] N. Masuda, K. Klemm, and V. M. Eguíluz, Phys. Rev. Lett. **111**, 188701 (2013).
[28] I. Belykh, M. di Bernardo, J. Kurths, and M. Porfiri, Physica D **267**, 1 (2014).
[29] M. Pósfai and P. Hövel, New J. Phys. **16**, 123055 (2014).
[30] B. C. McMeans, K. S. McCann, M. Humphries, N. Rooney, and A. T. Fisk, Trends Ecol. Evol. **30**, 662 (2015).
[31] B. Hou, X. Li, and G. Chen, IEEE Trans. Circuits Syst. I, Reg. Papers **63**, 1771 (2016).
[32] A. Li, S. P. Cornelius, Y. Y. Liu, L. Wang, and A. L. Barabási, Science **358**, 1042 (2017).
[33] J. Petit, B. Lauwens, D. Fanelli, and T. Carletti, Phys. Rev. Lett. **119**, 148301 (2017).
[34] M. Ushio, C.-H. Hsieh, R. Masuda, E. R. Deyle, H. Ye, C.-W. Chang, G. Sugihara, and M. Kondoh, Nature (London) **554**, 360 (2018).
[35] Z.-L. Hu, Z.-S. Shen, S.-N. Cao, B. Podobnik, H.-J. Yang, W.-X. Wang, and Y.-C. Lai, Sci. Rep. **8**, 2685 (2018).
[36] D. J. Stilwell, E. M. Bollt, and D. G. Roberson, SIAM J. Appl. Dyn. Syst. **5**, 140 (2006).
[37] M. Porfiri, D. J. Stilwell, E. M. Bollt, and J. D. Skufca, Physica D **224**, 102 (2006).
[38] M. Chen, Phys. Rev. E **76**, 016104 (2007).
[39] M. Porfiri, D. J. Stilwell, and E. M. Bollt, IEEE Trans. Circuits Syst. I, Reg. Papers **55**, 3170 (2008).
[40] L. Chen, C. Qiu, and H. B. Huang, Phys. Rev. E **79**, 045101(R) (2009).
[41] L. Wang, H. Shi, and Y.-X. Sun, Phys. Rev. E **82**, 046222 (2010).
[42] N. Fujiwara, J. Kurths, and A. Díaz-Guilera, Phys. Rev. E **83**, 025101(R) (2011).
[43] M. Porfiri, Phys. Rev. E **85**, 056114 (2012).
[44] S. H. Lee, S. Lee, S.-W. Son, and P. Holme, Phys. Rev. E **85**, 027202 (2012).
[45] B. Kim, Y. Do, and Y.-C. Lai, Phys. Rev. E **88**, 042818 (2013).
[46] Y. Guo, W. Lin, and D. W. C. Ho, Chaos **26**, 033113 (2016).
[47] M. Jiménez-Martín, J. Rodríguez-Laguna, O. D'Huys, J. de la Rubia, and E. Korutcheva, Phys. Rev. E **95**, 052210 (2017).
[48] S. Rakshit, B. K. Bera, D. Ghosh, and S. Sinha, Phys. Rev. E **97**, 052304 (2018).
[49] Y. Guo, W. Lin, and G. Chen, IEEE Trans. Autom. Control **63**, 21 (2018).
[50] S. Rakshit, B. K. Bera, and D. Ghosh, Phys. Rev. E **98**, 032305 (2018).
[51] K. P. O'Keeffe, J. H. M. Evers, and T. Kolokolnikov, Phys. Rev. E **98**, 022203 (2018).
[52] L. Gammaitoni, P. Hänggi, P. Jung, and F. Marchesoni, Rev. Mod. Phys. **70**, 223 (1998).
[53] W. Horsthemke and R. Lefever, *Noise-Induced Transition: Theory and Applications in Physics, Chemistry, and Biology* (Springer-Verlag, Berlin, 1984).
[54] W. Lin and G. Chen, Chaos **16**, 013134 (2006).
[55] O. Golovneva, R. Jeter, I. Belykh, and M. Porfiri, Physica D **340**, 1 (2017).
[56] L. M. Pecora and T. L. Carroll, Phys. Rev. Lett. **80**, 2109 (1998).
[57] L. Huang, Q. Chen, Y.-C. Lai, and L. M. Pecora, Phys. Rev. E **80**, 036204 (2009).
[58] W. Lu and T. Chen, Physica D **213**, 214 (2006).
[59] J. Sun, E. M. Bollt, and T. Nishikawa, Europhys. Lett. **85**, 60011 (2009).
[60] A. F. Karr, *Probability* (Springer-Verlag, New York, 1993).
[61] M. Viana and K. Oliveira, *Foundations of Ergodic Theory* (Cambridge University Press, Cambridge, UK, 2016).
[62] W. Feller, *An Introduction to Probability Theory and Its Applications*, 2nd ed. (John Wiley & Sons Inc., New York, 1971), Vol. II.
[63] E. Ott and T. M. Antonsen, Chaos **18**, 037113 (2008).
[64] J. B. Conway, *Functions of One Complex Variable*, 2nd ed. (Springer-Verlag, New York, 1978).
[65] S. Zhou, P. Ji, Q. Zhou, J. Feng, J. Kurths, and W. Lin, New J. Phys. **19**, 083004 (2017).
[66] A. M. Hagerstrom, T. E. Murphy, R. Roy, P. Hoevel, I. Omelchenko, and E. Schoell, Nat. Phys. **8**, 658 (2012).
[67] D. J. Watts and S. H. Strogatz, Nature (London) **393**, 440 (1998).
[68] I. J. Farkas, I. Derényi, A.-L. Barabási, and T. Vicsek, Phys. Rev. E **64**, 026704 (2001).
[69] N. F. Rulkov, Phys. Rev. Lett. **86**, 183 (2001).